SANDIA REPORT

SAND2012-7863
Unlimited Release
Printed September 2012

Transportation Energy Pathways LDRD

Garrett E. Barter, David Reichmuth, Jessica Westbrook, Leonard A. Malczynski, Ann S. Yoshimura, Meghan B. Peterson, Todd H. West, Dawn K. Manley, Katherine D. Guzman, Donna M. Edwards, Valerie A. Peters

Prepared by
Sandia National Laboratories
Albuquerque, New Mexico 87185 and Livermore, California 94550

Sandia National Laboratories is a multi-program laboratory managed and operated by Sandia Corporation, a wholly owned subsidiary of Lockheed Martin Corporation, for the U.S. Department of Energy's National Nuclear Security Administration under contract DE-AC04-94AL85000.

Sandia National Laboratories

Issued by Sandia National Laboratories, operated for the United States Department of Energy by Sandia Corporation.

Available to DOE and DOE contractors from
U.S. Department of Energy
Office of Scientific and Technical Information
P.O. Box 62
Oak Ridge, TN 37831

Telephone: (865) 576-8401
Facsimile: (865) 576-5728
E-Mail: reports@adonis.osti.gov
Online ordering: http://www.osti.gov/bridge

Available to the public from
U.S. Department of Commerce
National Technical Information Service
5285 Port Royal Rd
Springfield, VA 22161

Telephone: (800) 553-6847
Facsimile: (703) 605-6900
E-Mail: orders@ntis.fedworld.gov
Online ordering: http://www.ntis.gov/help/ordermethods.asp?loc=7-4-0#online

SAND2012-7863
Unlimited Release
Printed September 2012

Transportation Energy Pathways LDRD

Garrett E. Barter David Reichmuth Jessica Westbrook
Leonard A. Malczynski Ann S. Yoshimura Meghan B. Peterson
Todd H. West Dawn K. Manley Katherine D. Guzman Donna M. Edwards
Valerie A. Peters

Abstract

This report presents a system dynamics based model of the supply-demand interactions between the US light-duty vehicle (LDV) fleet, its fuels, and the corresponding primary energy sources through the year 2050. An important capability of our model is the ability to conduct parametric analyses. Others have relied upon scenario-based analysis, where one discrete set of values is assigned to the input variables and used to generate one possible realization of the future. While these scenarios can be illustrative of dominant trends and tradeoffs under certain circumstances, changes in input values or assumptions can have a significant impact on results, especially when output metrics are associated with projections far into the future. This type of uncertainty can be addressed by using a parametric study to examine a range of values for the input variables, offering a richer source of data to an analyst.

The parametric analysis featured here focuses on a trade space exploration, with emphasis on factors that influence the adoption rates of electric vehicles (EVs), the reduction of GHG emissions, and the reduction of petroleum consumption within the US LDV fleet. The underlying model emphasizes competition between 13 different types of powertrains, including conventional internal combustion engine (ICE) vehicles, flex-fuel vehicles (FFVs), conventional hybrids(HEVs), plug-in hybrids (PHEVs), and battery electric vehicles (BEVs).

We find that many factors contribute to the adoption rates of EVs. These include the pace of technological development for the electric powertrain, battery performance, as well as the efficiency improvements in conventional vehicles. Policy initiatives can also have a dramatic impact on the degree of EV adoption. The consumer effective payback period, in particular, can significantly increase the market penetration rates if extended towards the vehicle lifetime.

Widespread EV adoption can have noticeable impact on petroleum consumption and greenhouse gas (GHG) emission by the LDV fleet. However, EVs alone cannot drive compliance with the most aggressive GHG emission reduction targets, even as the current electricity source mix shifts away from coal and towards natural gas. Since ICEs will comprise the majority of the LDV fleet for up to forty years, conventional vehicle efficiency improvements have the greatest potential for reductions in LDV GHG emissions over this time. These findings seem robust even if global oil prices rise to two to three times current projections. Thus, investment in improving the internal combustion engine might be the cheapest, lowest risk avenue towards meeting ambitious GHG emission and petroleum consumption reduction targets out to 2050.

Acknowledgment

The authors would like to thank Dr. Andrew Lutz, Dr. Benjamin Wu, Prof. Joan Ogden and Dr. Christopher Yang for their suggestions over the course of this project. This work was funded by the Laboratory Directed Research and Development program at Sandia National Laboratories.

Contents

List of Figures

List of Tables

Nomenclature

Demand variables

$\mathbb{D}^E$	Energy source demand
$\mathbb{D}^F$	Fuel use demand
$\mathbb{D}^{F^P}$	Fuel production demand

Vehicle cost variables

$\mathbb{C}^G$	Generalized vehicle ownership cost
$\mathbb{C}^F$	Vehicle fuel costs
$\mathbb{C}^B$	Electric vehicle battery capital cost
$\mathbb{C}^H$	Electric vehicle charger cost
$\mathbb{C}^P$	Penalty costs
$\mathbb{C}^V$	Vehicle capital cost minus battery
$\mathbb{C}^Y$	Electric vehicle subsidy
δ	Dollar cost constant
$\mathbf{A}(\cdot)$	Amortization function

Logit choice variables

$\mathcal{U}^V$	Vehicle logit choice utility
$\mathcal{U}^F$	Flex fuel logit choice utility
$\mathcal{U}^R$	EtOH production state logit choice utility
β	Logit choice exponent
$\mathbb{C}_0$	Reference cost
$\mathbb{P}_0$	Reference price

Subscript segmentation

a	Subscript for vehicle age
d	Subscript for driving intensity
e	Subscript for energy source
f	Subscript for fuel
h	Subscript for housing type
n	Subscript for vehicle powertrain
p	Subscript for population density
r	Subscript for geographic region
s	Subscript for vehicle size class

Gamma distribution variables

$\Gamma(\cdot)$	Gamma function
$\gamma(\cdot)$	Lower incomplete gamma function
k	Shape parameter
θ	Scale parameter

Price variables

$\mathbb{P}^E$	Energy source price
$\mathbb{P}^F$	Fuel price
$\mathbb{P}^C$	Price for carbon emissions

Vehicle fleet variables

$\mathcal{V}$	Number of vehicles
$\mathcal{S}$	Overall vehicle sales rate
$\mathcal{W}$	Overall vehicle scrap rate
σ	Segment sales fraction
ω	Segment scrap fraction
$\mathcal{Q}$	Charger cost reduction rate
$\mathcal{R}$	Vehicle range
$\mathcal{M}$	Annual VMT
η	Vehicle fuel economy
ρ	Vehicle fuel use rate
Φ	Number of refueling stations
ϕ	Refueling station fraction
κ	Market availability fraction
m^0	Market introduction year
α	Number of new stations per vehicle sold
ν	FFV fuel choice based on price

Fuel production variables

Ω^F	Energy source to fuel conversion rate
$\mathcal{G}$	CO_2-equivalent GHG emissions
λ^F	GHG emission rate for fuel use
λ^C	GHG emission rate for fuel conversion
τ	Regional fuel exchange matrix
η^F	Fuel economy for tanker transport
$\mathcal{X}$	Regional fuel exchange distance
$\mathcal{T}$	Taxes, fees, and profit margin
$\mathcal{E}$	Energy source price multiplier
L	Electricity generator lifetime
$\mathcal{Y}$	Electricity generation capacity
$\mathcal{Z}$	Base electricity demand
Ω^E	Energy source to electricity conversion rate
$\mathcal{C}^{Cap}$	New electricity generation capital cost
$\mathcal{C}^{OM}$	New electricity generation O&M cost
ψ	New electricity generation source type

Abbreviations

ICE	Internal combustion engine
AFV	Alternative fuel vehicle
FFV	Flex fuel vehicle
EV	Electric vehicle
HEV	Hybrid electric vehicle
PHEV	Plug-in hybrid electric vehicle
BEV	Battery electric vehicle
LDV	Light duty vehicle
GHG	Greenhouse gas
VMT	Vehicle miles traveled
GGE	Gallon gasoline equivalent
CNG	Compressed natural gas

Chapter 1

Introduction

The objective of this project was to parameterically assess the value and viability of electric light-duty vehicles (LDVs) in the United States. Specifically, the project was interested in understanding the set of market, technology, policy, and economic charasterictics that could drive adoption of electric vehicles and/or lead to notable reductions in fleet greenhouse gas emissions and fuel consumption. To address these questions, this project developed a system dynamics based model of the interactions between the US LDV fleet, its fuels, and the corresponding raw energy sources through the year 2050. The differentiating feature of the model is the ability to conduct parametric analyses. Others have relied upon scenario-based analysis, where one discrete set of values is assigned to the input variables and used to generate one possible realization of the future [2, 13, 20, 24]. In these studies, there is often a *reference* case, as well as perhaps *optimistic* and *pessimistic* perturbation scenarios relative to the reference case. While these scenarios can be illustrative of dominant trends and tradeoffs under certain circumstances, changes in input values or assumptions can have a significant impact on results, especially when output metrics are associated with projections far into the future. For instance, two similar models at Argonne National Laboratories arrived at significantly different predictions of LDV oil consumption in 2050 due to the fact that one was calibrated to reference input values published in 2007 and another was calibrated to 2008 data [24]. This type of uncertainty can be addressed by using a parametric study to examine a range of values for the input variables, offering a richer source of data to an analyst. It also enables a sensitivity analysis, which can reveal the underlying sources of uncertainty in a model, as well as identify key drivers of output metrics. Additionally, the n-dimensional shape of the trade space can be characterized to locate points of interest, such as iso-performance contours that trace the multiple sets of parameter values that can be used to achieve performance goals. The analysis approach, results, and an earlier version of the model were published in Barter et al. [3].

This report is divided into five chapters, following this introduction. Next is a detailed decription of the parametric model, its methodology, assumptions, and data sources. Chapter 3 presents the numerical results, focusing first on a global sensitivity analysis of the model to give greater insight into its behavior and the key drivers of uncertainty. This chapter also includes a discussion of one- and two-parameter variation studies used to understand the trade space for the impact of the US LDV fleet characteristics and associated policies on GHG emissions and petroleum consumption. This is followed by a short chapter of concluding comments following the analysis.

In addition to the primary project objective, a related effort was also executed under the auspices of this LDRD. This task was an assessment of fuel economy for construction vehicles, which was published as Peters and Manley [23]. Chapter 5 provides a brief summary of this work.

This page intentionally left blank.

Chapter 2

Model description

This chapter presents a detailed description of the modeling approach, key assumptions, model equations, and data sources.

Our model is implemented using a system dynamics approach to construct a set of interacting algebraic and differential equations using Python and the Numpy library (early versions of the model, including that used in Barter et al. [3], were constructed using Powersim Studio, a visual programming environment for system dynamics). Solutions are generated using a third-order Runge-Kutta algorithm with fixed step size. A high-level diagram of the model components is shown in Figure 2.1. The model is broken down into four modules: an energy supply sub-model, a fuel production sub-model, an electricity grid sub-model, and a vehicle sub-model. The sub-models exchange price and demand points for energy supply stock and fuels.

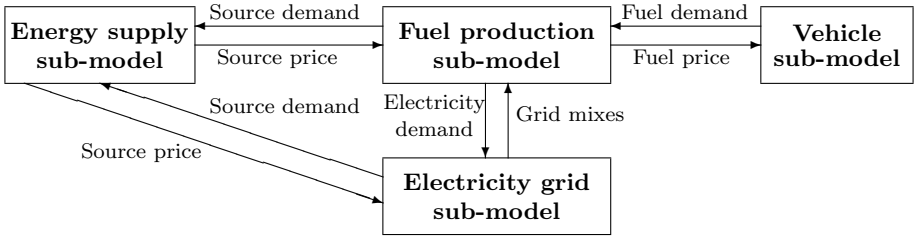

Figure 2.1. High-level diagram of the model components.

The model is initialized with a distribution of existing vehicles representative of the current fleet and then calculates annual vehicle sales and scrapping to determine the evolution of the fleet composition. The sales rate of each vehicle is determined using a choice algorithm that considers vehicle purchase cost, fuel costs, and penalty factors (e.g. range penalties). The cost of fuels and vehicles depends, in part, on the demand and prior sales so that there are both positive and negative feedback effects on the vehicle sales rate. The model tracks vehicles and fuel use in the 48 states of the continental United States, as well as the District of Columbia. Fuel demand is negotiated with supply using raw energy supply curves at a global, national, or state scale, depending on the energy stock.

2.1 Vehicle modeling

2.1.1 Vehicle segmentation

The model starts in 2010 with 232 million light-duty vehicles in service in the United States. The initial vehicle fleet is segmented by age, geographic region, vehicle size, vehicle powertrain, population density,

driving intensity, and owner housing type,

$$\mathcal{V} = \mathcal{V}_{arsnpdh} \quad .$$

The subscripts, which will be used throughout the model description, denote segmentation by a age, r region, s vehicle size, n powertrain, p population density, d driving intensity, and h housing type.

Overall sales and scrap rates are kept at a constant percent of fleet size, with sales at 6.7% and scrap rate at 5.8%. The sales rate used is the average sales rate for the period 2000-2009 [6]. The overall number of vehicles increases at 0.9% per year, the average rate of projected population growth from 2010 through 2050, and thus assumes no change in the number of vehicles per capita [4]. While the overall rate of vehicle scrapping is fixed, the scrap rate of vehicles increases as the vehicles age, using rates derived from survival data [35]. Because only new car sales and final disposal of the vehicles are considered, used vehicle sales are not tracked. The evolution of each vehicle segment is therefore given by,

$$\frac{\mathrm{d}\mathcal{V}_{a=0,rsnpdh}}{\mathrm{d}t} = \sigma_{rsnpdh}\mathcal{S}\sum_{an}\mathcal{V}_{arsnpdh}$$

$$\frac{\mathrm{d}\mathcal{V}_{arsnpdh}}{\mathrm{d}t} = -\omega_{sa}\mathcal{W}\mathcal{V}_{arsnpdh}$$

where $\mathcal{S}$ is the overall sales rate, $\mathcal{W}$ is the overall scrap rate, ω is the scrap fraction taken from survival data, and σ is the consumer sales fraction by powertrain for each vehicle segment such that,

$$\sum_{n}\sigma_{rsnpdh} = 1 \quad .$$

The components of each vehicle segment are,

- Age
  - 0-46 years
- Geographic region
  - 48 states in the continental United States
  - District of Columbia
- Vehicle size
  - Compact
  - Midsize
  - Small SUV
  - Large SUV
  - Light pickup
- Vehicle powertrain
  - Gasoline-fueled Spark Ignition (SI) vehicle
  - Diesel-fueled Compression Ignition (CI) vehicle
  - E85 Flex-Fuel vehicle (FFV)
  - SI Hybrid electric vehicle (HEV)
  - CI HEV
  - E85 HEV
  - SI Plugin Hybrid Electric Vehicle (PHEV) with 10 mile all-electric range (SIPHEV10)

  - CI PHEV 10
  - E85 PHEV 10
  - SI PHEV 40
  - CI PHEV 40
  - E85 PHEV 40
  - Battery-electric vehicle (BEV) with 150 mile all-electric range (BEV150)
  - Compressed natural gas (CNG) vehicle
  - CNG-Gasoline bi-fuel vehicle (CNGBI)
  - Hydrogen fuel cell vehicle
- Population density
  - Urban
  - Suburban
  - Rural
- Driver intensity
  - Light
  - Medium
  - Heavy
- Owner housing type
  - Single family house with natural gas
  - Single family house without natural gas
  - Other

The number of initial vehicles segmented by vehicle size and state is taken from vehicle registration data [33]. The age distribution is incorporated from the US Department of Transportation [35] based on survival data and is listed in Table 2.2. These initial vehicles are primarily SI powertrains, but E85, CI, and SIHYBRID powertrain vehicles exist as well. The numbers of the alternative vehicles in the initial fleet is based on sales data and state based reporting of hybrid sales [6]. The fleet is further segmented by population density and home housing type, based on census data [4], shown in Table 2.3. Finally, the vehicle fleet is segmented by binning driving intensity which relates to an average daily trip distance expressed by a gamma distribution. The bins and gamma distribution parameters for the driving intensity segmentation are shown in Table 2.5. Through the National Highway Travel Survey data set, population density is also related to vehicle size and driver intensity [34], shown in Table 2.4. For reference, the gamma distribution has a cumulative distribution function of the form,

$$F(x; k, \theta) = \frac{\gamma(x, \frac{k}{\theta})}{\Gamma(k)},$$

where $\gamma(\cdot)$ is the lower, incomplete gamma function, $\Gamma(\cdot)$ is the gamma function, k is the shape parameter, and θ is the scale parameter [14].

We assume that the annual vehicle mileage traveled (VMT) is constant for each segment over the course of the simulation. The variation of VMT over vehicle size, region, and population density is initialized using the *BESTMILE* estimate of the National Highway Travel Survey [34]. These averages are apportioned to vehicle age, to reflect decreasing annual miles as vehicles age [35], and also to driving intensity using the gamma distribution bins listed above.

Table 2.1. Initial vehicles by state and size [33].

State	Compact	Midsize	Small SUV	Large SUV	Pickup
Alabama	1,144,982	1,009,265	540,162	486,154	1,237,499
Arizona	1,174,697	1,035,458	594,218	561,339	865,059
Arkansas	498,265	439,205	251,981	231,701	576,242
California	10,501,828	9,257,020	3,878,625	4,004,211	4,969,372
Colorado	334,951	295,249	229,392	182,767	253,844
Connecticut	1,047,722	923,533	371,362	367,396	302,744
Delaware	242,450	213,711	44,258	43,837	49,175
District of Columbia	86,182	75,966	15,886	15,629	5,495
Florida	3,974,990	3,503,825	1,899,107	1,961,938	2,023,580
Georgia	2,180,370	1,921,925	1,153,104	1,106,241	1,714,689
Idaho	295,712	260,660	160,550	147,149	412,231
Illinois	3,054,415	2,692,368	1,224,637	1,432,567	1,159,392
Indiana	1,652,893	1,456,972	598,119	805,116	1,033,378
Iowa	917,702	808,924	299,305	401,459	719,390
Kansas	460,698	406,091	268,624	439,695	644,428
Kentucky	1,023,359	902,057	352,317	381,447	783,064
Louisiana	999,522	881,047	477,708	413,788	1,066,072
Maine	282,820	249,296	121,559	122,922	236,524
Maryland	1,373,003	1,210,258	622,329	656,975	534,683
Massachusetts	1,651,104	1,455,395	744,467	735,828	567,152
Michigan	2,296,373	2,024,178	991,681	1,201,188	1,175,330
Minnesota	1,324,834	1,167,798	517,059	649,205	825,675
Mississippi	607,339	535,349	180,820	167,378	471,777
Missouri	1,356,231	1,195,473	555,414	619,499	1,006,428
Montana	193,184	170,286	102,320	93,319	259,884
Nebraska	408,609	360,175	204,387	222,527	385,697
Nevada	370,308	326,414	190,108	157,414	238,339
New Hampshire	337,567	297,554	161,892	157,930	220,562
New Jersey	1,947,011	1,716,227	882,650	901,178	476,719
New Mexico	362,339	319,390	201,958	178,974	432,155
New York	4,594,344	4,049,765	797,072	869,997	527,854
North Carolina	1,816,635	1,601,305	638,365	653,627	1,001,881
North Dakota	182,345	160,731	62,072	71,647	168,866
Ohio	3,320,291	2,926,729	1,212,175	1,511,354	1,584,804
Oklahoma	880,427	776,068	320,501	320,571	828,890
Oregon	748,999	660,218	383,977	394,482	665,324
Pennsylvania	3,068,907	2,705,142	1,215,599	1,258,304	1,174,895
Rhode Island	253,485	223,438	97,813	101,571	86,996
South Carolina	1,043,083	919,444	435,958	419,450	685,266
South Dakota	211,062	186,045	93,929	105,993	218,296
Tennessee	1,504,966	1,326,578	561,946	556,304	1,013,682
Texas	4,630,069	4,081,255	2,401,983	2,131,902	4,192,574
Utah	640,443	564,529	321,365	296,559	495,699
Vermont	153,665	135,451	71,736	66,131	110,339
Virginia	1,966,673	1,733,559	758,336	771,111	876,819
Washington	1,637,225	1,443,161	631,520	657,495	1,002,271
West Virginia	365,120	321,841	166,811	152,733	328,388
Wisconsin	1,334,050	1,175,922	554,820	712,897	821,490
Wyoming	110,300	97,226	91,636	73,019	232,144

Table 2.2. Vehicle lifetime survival fraction as a function of age and size [35].

Vehicle age	**Fraction Surviving to Age**				
[years]	Compact	Midsize	Small SUV	Large SUV	Light truck
0	1.00	1.00	1.00	1.00	1.00
1	0.99	0.99	0.99	0.98	0.97
2	0.98	0.98	0.98	0.97	0.96
3	0.97	0.97	0.97	0.96	0.94
4	0.96	0.96	0.96	0.94	0.92
5	0.94	0.94	0.94	0.92	0.89
6	0.92	0.92	0.92	0.89	0.86
7	0.89	0.89	0.89	0.86	0.82
8	0.86	0.86	0.86	0.82	0.78
9	0.83	0.83	0.83	0.78	0.74
10	0.79	0.79	0.79	0.74	0.70
11	0.72	0.72	0.72	0.68	0.65
12	0.61	0.61	0.61	0.61	0.60
13	0.51	0.51	0.51	0.53	0.55
14	0.41	0.41	0.41	0.46	0.50
15	0.33	0.33	0.33	0.39	0.45
16	0.26	0.26	0.26	0.33	0.41
17	0.20	0.20	0.20	0.28	0.36
18	0.16	0.16	0.16	0.24	0.32
19	0.12	0.12	0.12	0.20	0.29
20	0.09	0.09	0.09	0.17	0.25
21	0.07	0.07	0.07	0.15	0.22
22	0.05	0.05	0.05	0.13	0.20
23	0.04	0.04	0.04	0.11	0.17
24	0.03	0.03	0.03	0.09	0.15
25	0.02	0.02	0.02	0.08	0.13
26	0.02	0.02	0.02	0.07	0.12
27	0.01	0.01	0.01	0.06	0.10
28	0.00	0.00	0.00	0.05	0.09
29	0.00	0.00	0.00	0.04	0.08
30	0.00	0.00	0.00	0.04	0.07
31	0.00	0.00	0.00	0.03	0.06
32	0.00	0.00	0.00	0.03	0.05
33	0.00	0.00	0.00	0.02	0.04
34	0.00	0.00	0.00	0.02	0.04
35	0.00	0.00	0.00	0.02	0.03
36	0.00	0.00	0.00	0.01	0.03
37	0.00	0.00	0.00	0.01	0.03
38	0.00	0.00	0.00	0.01	0.02
39	0.00	0.00	0.00	0.00	0.02
40	0.00	0.00	0.00	0.00	0.02
41	0.00	0.00	0.00	0.00	0.01
42	0.00	0.00	0.00	0.00	0.01
43	0.00	0.00	0.00	0.00	0.01
44	0.00	0.00	0.00	0.00	0.00
45	0.00	0.00	0.00	0.00	0.00

Table 2.3. State population density and housing type fractions (SF is *single family house*) [4].

State	Population Density			Housing Type		
	Urban	Suburban	Rural	SF w/o NG	SF w/ NG	Other
Alabama	0.27	0.28	0.45	0.30	0.37	0.32
Arizona	0.64	0.23	0.13	0.29	0.35	0.36
Arkansas	0.22	0.30	0.48	0.30	0.37	0.32
California	0.66	0.27	0.07	0.29	0.35	0.36
Colorado	0.52	0.30	0.18	0.29	0.35	0.36
Connecticut	0.35	0.52	0.12	0.25	0.31	0.44
Delaware	0.13	0.67	0.20	0.30	0.37	0.32
District of Columbia	1.00	0.00	0.00	0.30	0.37	0.32
Florida	0.36	0.54	0.11	0.30	0.37	0.32
Georgia	0.21	0.49	0.29	0.30	0.37	0.32
Idaho	0.31	0.33	0.36	0.29	0.35	0.36
Illinois	0.42	0.46	0.13	0.32	0.39	0.29
Indiana	0.33	0.39	0.28	0.32	0.39	0.29
Iowa	0.27	0.35	0.39	0.32	0.39	0.29
Kansas	0.35	0.36	0.29	0.32	0.39	0.29
Kentucky	0.17	0.39	0.44	0.30	0.37	0.32
Louisiana	0.36	0.36	0.28	0.30	0.37	0.32
Maine	0.09	0.28	0.63	0.25	0.31	0.44
Maryland	0.30	0.57	0.14	0.30	0.37	0.32
Massachusetts	0.40	0.51	0.09	0.25	0.31	0.44
Michigan	0.35	0.37	0.28	0.32	0.39	0.29
Minnesota	0.28	0.40	0.32	0.32	0.39	0.29
Mississippi	0.13	0.35	0.51	0.30	0.37	0.32
Missouri	0.28	0.40	0.32	0.32	0.39	0.29
Montana	0.22	0.30	0.48	0.29	0.35	0.36
Nebraska	0.36	0.32	0.32	0.32	0.39	0.29
Nevada	0.74	0.16	0.09	0.29	0.35	0.36
New Hampshire	0.20	0.35	0.44	0.25	0.31	0.44
New Jersey	0.20	0.74	0.05	0.25	0.31	0.44
New Mexico	0.38	0.36	0.26	0.29	0.35	0.36
New York	0.53	0.33	0.14	0.25	0.31	0.44
North Carolina	0.28	0.31	0.41	0.30	0.37	0.32
North Dakota	0.30	0.24	0.46	0.32	0.39	0.29
Ohio	0.30	0.49	0.21	0.32	0.39	0.29
Oklahoma	0.36	0.29	0.35	0.30	0.37	0.32
Oregon	0.37	0.41	0.22	0.29	0.35	0.36
Pennsylvania	0.23	0.53	0.24	0.25	0.31	0.44
Rhode Island	0.38	0.53	0.09	0.25	0.31	0.44
South Carolina	0.14	0.47	0.39	0.30	0.37	0.32
South Dakota	0.23	0.28	0.48	0.32	0.39	0.29
Tennessee	0.35	0.29	0.36	0.30	0.37	0.32
Texas	0.51	0.29	0.19	0.30	0.37	0.32
Utah	0.41	0.45	0.15	0.29	0.35	0.36
Vermont	0.06	0.28	0.66	0.25	0.31	0.44
Virginia	0.34	0.37	0.29	0.30	0.37	0.32
Washington	0.37	0.44	0.19	0.29	0.35	0.36
West Virginia	0.13	0.34	0.54	0.30	0.37	0.32
Wisconsin	0.30	0.35	0.34	0.32	0.39	0.29
Wyoming	0.20	0.42	0.38	0.29	0.35	0.36

Table 2.4. Distribution of vehicle size in population density segments [34].

	Vehicle size				
Population density	Compact	Midsize	Small SUV	Large SUV	Light truck
Urban	0.326	0.287	0.137	0.143	0.107
Suburban	0.304	0.268	0.145	0.153	0.129
Rural	0.241	0.213	0.142	0.143	0.262

Table 2.5. Segmentation of driving intensity in each population density segment and the associated gamma distribution of daily driving distance [14].

Driving	**Population density**			**Gamma distribution**	
intensity	Urban	Suburban	Rural	k	θ
Light	40%	37%	27%	1.68	14.11
Medium	34%	31%	33%	1.90	23.20
Heavy	26%	31%	40%	1.80	43.05

Table 2.6. Fraction of miles driven on liquid fuel or electricity (fuel use rates). Note that serial drive train mode is assumed for PHEVs (vehicles use electricity up to the electric powertrain range limit and then liquid fuel only).

Driving	**PHEV10**		**PHEV40**	
intensity	Liquid	Electricity	Liquid	Electricity
Light	42%	58%	4%	96%
Medium	63%	37%	17%	83%
Heavy	76%	24%	35%	65%

Table 2.7. US light-duty vehicle mass market introduction year for each powertrain.

Powertrain	**Year**	**Powertrain**	**Year**	**Powertrain**	**Year**
SI	1930	SIPHEV10	2012	BEV150	2011
CI	2008	CIPHEV10	2025	CNG	2013
E85	2001	E85PHEV10	2018	CNGBI	2014
SIHEV	2000	SIPHEV40	2011	H2FC	2020
CIHEV	2020	CIPHEV40	2025		
E85HEV	2015	E85PHEV40	2013		

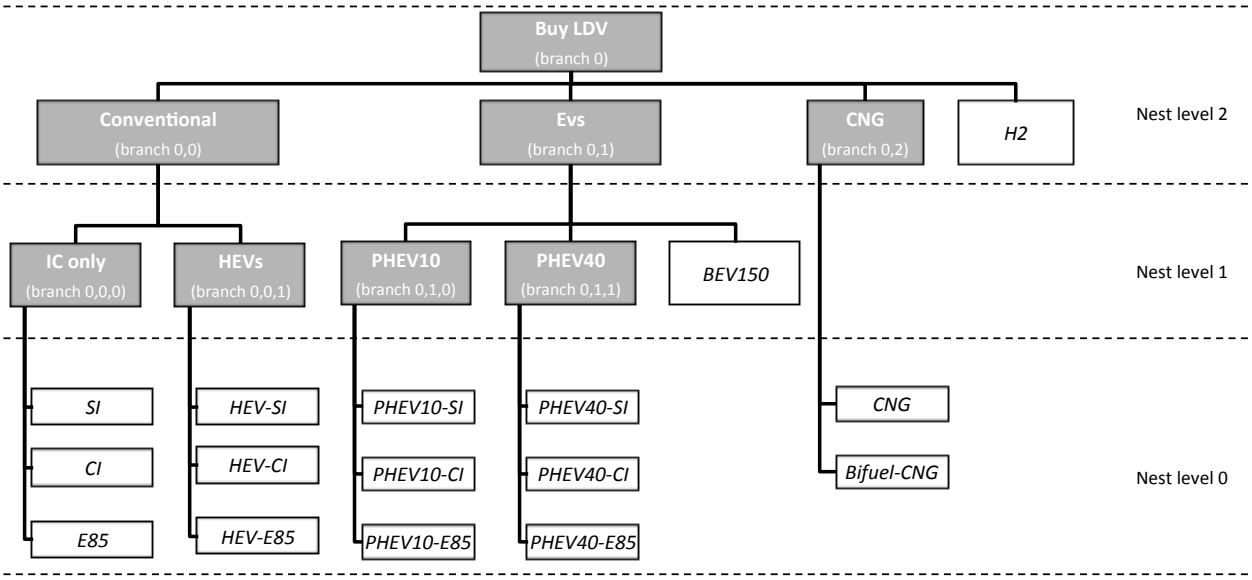

Figure 2.2. Nested consumer choice diagram.

Initial vehicles in the fleet are assigned fuel efficiency based on historical data [37]. Future vehicle efficiency data for all powertrains and all fuel sources are taken from an ANL-led study for DOE [19]. These efficiencies also comply with the regulatory targets proposed by the U.S. Environmental Protection Agency and U.S. Department of Transportation [38]. The same source also provides battery capacity for all of the hybrid, plug-in hybrid, and battery electric vehicles as a function of time. The amount of electricity versus liquid fuel used by the PHEVs is determined by the cumulative distribution function value of the electric range for the segment average daily driving pattern [8]. PHEV vehicles are thus assumed to operate in a serial drive train mode with daily home recharging, such that only on-board electricity is used when daily driving is less than the battery range. These electricity use rates are shown in Table 2.6.

2.1.2 Vehicle purchase model

The segment sales fractions in each time-step, σ, are assigned using a nested logit choice model, similar to Lin and Greene [18] and Struben and Sterman [28]. Aside from the choice of powertrain, we do not assume the migration of consumers from one segment to another, including vehicle size. The nests are shown in Figure 2.2 and are evaluated from the bottom-up. The sales fraction for a given segment is given by,

$$\sigma_{rsnpdh} = \kappa_n \prod_{i=0}^{2} \sigma^i_{rsnpdh};$$

$$\kappa_n = \frac{k_1}{1 + 1000 \exp\left[k_2(t - m^0_n)\right]}; \qquad k_1 = \begin{cases} 1, & t \geq m^0_n \\ 0, & t < m^0_n \end{cases}; \qquad k_2 = -0.35/\text{year}$$

where κ is the market availability fraction, the superscript i denotes the nest branch, σ^i is the sales fraction of the intermediate nest branches, and m^0 is the market introduction year of a given powertrain. The market availability fraction represents a growth curve tracking the availability of a given powertrain in vehicle manufacturers' fleets. The start year parameter for each powertrain (not necessarily the first year of

market introduction), m^0, is given in Table 2.7. The intermediate sales fractions are evaluated as,

$$\sigma^i_{rsnpdh} = \frac{\mathcal{U}^V_{rsnpdh}\sigma^{i-1}_{rsnpdh}}{\sum_{n\in i}\mathcal{U}^V_{rsnpdh}\sigma^{i-1}_{rsnpdh}}; \qquad \mathcal{U}^V_{rsnpdh} = \exp\left(-\beta^i \frac{\mathbb{C}^G_{rsnpdh}}{\mathbb{C}^G_0}\right); \tag{2.1}$$

where $\mathcal{U}^V$ is the utility, β^i is the logit exponent of the nest branch, $\mathbb{C}^G$ is the total cost, and $\mathbb{C}^G_0$ is a reference cost taken as the average of all initial vehicle segment costs. The sales fractions for nest level 0 are evaluated assuming $\sigma^{i-1} = 1$. The logit exponent values vary by *level*, as depicted in Figure 2.2. The baseline values, from the lowest to highest nest levels are, $\beta = [15, 12, 9]$, which are calibrated to give a price elasticity of -9 (a 9% drop in demand for a 1% increase in price) at a market share of 50% in nest level 0[12].

The generalized vehicle purchase costs, including penalties and subsidies, are amortized over a payback period and converted to a per mile cost using the annual vehicle miles traveled [15].

$$\mathbb{C}^G_{rsnpdh} = \mathbf{A}\left(\frac{\mathbb{C}^B_{sn} + \mathbb{C}^H_{nh} + \mathbb{C}^V_{sn} + \mathbb{C}^P_{rsnpdh} - \mathbb{C}^{Y^1}_{rsnpdh}}{\mathcal{M}_{a=0,rspd}}\right) + \mathbb{C}^F_{rsnpdh} - \frac{\mathbb{C}^{Y^2}_{rsnpdh}}{\mathcal{M}_{a=0,rspd}}, \tag{2.2}$$

where $\mathbb{C}^P$ is the penalty costs, $\mathbb{C}^B$ is the battery cost, $\mathbb{C}^H$ is the charger cost, $\mathbb{C}^V$ is the vehicle capital cost, $\mathbb{C}^F$ is the fuel cost per mile, $\mathbb{C}^Y$ is the value of subsidies, and $\mathcal{M}$ is the VMT. The function, $\mathbf{A}(\cdot)$, amortizes the cost to the consumer over a payback period of 3 years (in the baseline case) at a 0% discount rate. $\mathbb{C}^{Y,1}$ are national and state subsidies that are realized once, when the customer purchases a vehicle, and $\mathbb{C}^{Y,2}$ are recurring subsidies, such as fuel discounts or recurring tax rebates. The list of federal and state-based subsidies and incentives is lengthy and is compiled by the U.S. Department of Energy [30]. The individual cost components are discussed in the following paragraphs.

Vehicle purchase costs, $\mathbb{C}^V$, are calculated using estimates for advanced technology from Moawad et al. [19]. The costs include learning over time that captures the decline in manufacturing costs due to process and technological maturation. The cost for the batteries in electrified vehicles, $\mathbb{C}^B$, and the battery capacity in each vehicle, are also taken from the same source, but are included separately from other purchase costs so that the effect of targeted research in this area can be explored parametrically.

For vehicles that require home recharging, we include a charger cost with each vehicle,

$$\mathbb{C}^H_{nh} = \delta^H_{nh}\left(1-Q\right)^t; \qquad \delta^H_{nh} = \begin{cases} \$878, & \text{PHEV10 in single family house} \\ \$2146, & \text{PHEV40, BEV in single family house} \\ \$0, & \text{else} \end{cases},$$

where Q is the rate of price decline per year and t is the years since 2010. The charger cost assumes a Level 1 charger for PHEV10s and a Level 2 charger for PHEV40s and BEVs.

Penalty costs, $\mathbb{C}^P$, are also included to quantify limitations of alternative powertrains. A range penalty represents the reduced utility of a vehicle with a short range and is calculated using the value of the time spent refueling per daily mileage. A station availability penalty captures the lower utility of a vehicle that has limited public refueling options. The penalties are expressed as,

$$\mathbb{C}^P_{rsnpd} = \mathbb{C}^{P^1}_{snd} + \mathbb{C}^{P^2}_{rnp}$$

$$\mathbb{C}^{P^1}_{rsnpd} = \delta^{P^1}_n \frac{\mathcal{M}_{a=0,rspd}}{365\mathcal{R}_n}; \quad \delta^{P^1}_n = \begin{cases} \$532, & \text{BEV} \\ \$814, & \text{else} \end{cases}, \quad \mathcal{R}_n = \begin{cases} 150\,\text{mi}, & \text{BEV} \\ 350\,\text{mi}, & \text{else} \end{cases}$$

$$\mathbb{C}^{P^2}_{rnph} = \delta^{P^2}_{nh}\exp\left(-20.15\phi_{rnp}\right); \quad \delta^{P^2}_{nh} = \begin{cases} \$375, & \text{EVs in single family house} \\ \$7500, & \text{else} \end{cases}$$

where $\mathbb{C}^{P^1}$ is the range penalty, $\mathbb{C}^{P^2}$ is the refueling penalty, $\mathcal{R}$ is the vehicle range, and ϕ is the ratio of public fueling stations for an alternative powertrain to gasoline fueling stations in a given area. The cost

constant dollar values of the penalties, $\delta_n^{P^1}$ and $\delta_n^{P^2}$, are taken from Greene [12]. The growth trends of refueling infrastructure for alternative vehicles is taken from Yeh [41], which assumes new refueling stations are added as new alternative vehicles are built,

$$\frac{\mathrm{d}\Phi_{rpf}}{\mathrm{d}t} = \alpha \sum_{sdh,n\in f} \frac{\mathrm{d}\mathcal{V}_{a=0,rsnpdh}}{\mathrm{d}t}; \qquad \phi_{rnp} = \frac{\sum_{f\in n} \Phi_{rpf}}{\Phi_{rp,f=gas}},$$

where Φ is the number of refueling stations for a given fuel, α is the rate of new stations added per new vehicle sold, and the f subscript denotes type of fuel. The initial refueling station distribution by region and fuel type is taken from U.S. Department of Energy [32].

The fuel cost per mile, $\mathbb{C}^F$, is simply the product of the fuel price and the fuel consumption per mile of a vehicle,

$$\mathbb{C}^F_{rsdn} = \sum_f \frac{\mathbb{P}^F_{rhf}\rho_{rnpdhf}}{\eta_{a=0,snf}},$$

where $\mathbb{P}^F$ is the price of fuel, ρ is the fuel use rate, and η is the fuel economy.

2.1.3 Total fuel demand and FFVs

As shown in Figure 2.1, the vehicle sub-model outputs the total fuel use demand, $\mathbb{D}^F$. This is computed by an accounting of the total mileage covered by the fleet, the fuel use rates, and the fuel economy,

$$\mathbb{D}^F_{rf} = \sum_{asnpdh} \frac{\mathcal{V}_{arsnpdh}\mathcal{M}_{arspd}\rho_{rnpdhf}}{\eta_{asnf}} \quad .$$

The fuel use rate for most powertrains is static, with the breakdown between electricity and liquid fuel for the PHEVs shown in Table 2.6. However, the E85 flex-fuel vehicles can use either the ubiquitous E10 or the more limited E85 gasohol blends. The use rate of E85 versus E10 is dynamic and a function of the likelihood of visiting a station with an E85 pump and a choice by the consumer based on price per unit energy density. The choice model is of the same form as Equation 2.1, with an exponent value of $\beta^F = 18$,

$$\rho_{rpdh,n\in f=E85} = \phi_{rnp}\nu_{rh}; \qquad \nu_{rh} = \frac{\mathcal{U}^F_{rh,E85}}{\mathcal{U}^F_{rh,E10} + \mathcal{U}^F_{rh,E85}}; \qquad \mathcal{U}^F_{rhf} = \exp\left(-\beta^F \frac{\mathbb{P}^F_{rf}}{\mathbb{P}_0}\right) \quad ,$$

where ν is the E85 logit choice rate based on price, $\mathcal{U}^F$ is the logit choice utility, and the reference price, $\mathbb{P}_0$ is taken as the average of initial fuel prices.

2.2 Modeling fuel production and distribution

The fuel module calculates the cost and energy source mix of transportation fuels, given fuel demand from the vehicle model and energy source costs from the energy source sub-model. The module deconstructs the demand for pump-fuel blends consumers use, such as E10 and E85, into pure fuel demand. The set of pure fuels considered in the model are motor gasoline, diesel, ethanol, compressed natural gas, hydrogen, and electricity. The fuel derived demand in each state is matched with the corresponding raw energy feedstocks using conversion efficiencies specified by Wang [39]. State-by-state pricing variations are enforced for gasoline, diesel, and natural gas due to the complexities of the supply and refining network for those fuels. Ethanol may be transported from one state to another to satisfy extreme supply or cost imbalances due to the uneven distribution of biomass through the continental US. Well-to-pump GHG emissions are

computed using process estimates from Wang [39]. Pump-to-tailpipe GHG emissions are computed using the CO_2-equivalent content of the fuel and the total fuel demand.

The Renewable Fuel Standard (RFS) [22, 27, 40] is moderately enforced, in that the ethanol fraction by volume in the gasohol blendstock is assumed to rise to satisfy increased use of ethanol in transportation. However, this rise is capped at E15 due to skepticism that higher blend levels will be allowed. Furthermore, the quantity of ethanol produced from corn and other grains, as specified by RFS, is assumed to be satisfied first before other types feedstocks. Ethanol demand beyond the grain-based RFS limits is assumed to come from cellulosic sources. We do not currently track advanced, drop-in biofuel replacements for gasoline or biodiesel.

The ethanol supply state for each region is chosen by a logit choice function of the same form as Equation 2.1, with an exponent value of $\beta^R = 18$,

$$\tau_{rr',f=EtOH} = \frac{\mathcal{U}^R_{rr'}}{\sum_{r'} \mathcal{U}^R_{rr'}}; \qquad \mathcal{U}^R_{rr'} = \exp\left(-\beta^R \frac{\mathbb{P}^{F^P}_{rr',f=EtOH}}{\mathbb{P}_0}\right); \qquad \mathbb{P}^{F^P}_{rr'f} = \mathbb{P}^F_{rf} + \frac{\mathcal{X}_{rr'}}{\eta^F}\left(\mathbb{P}^F_{r,diesel} + \mathbb{P}^C \lambda^F_{diesel}\right),$$

where τ is the inter-region ethanol exchange matrix from production state, r, to demand state, r', $\mathbb{P}^{F^P}$ is the fuel price after state exchange is accounted for, $\mathcal{X}$ is the distance between state centroids, η^F is the fuel economy of the transport mode (taken to be the average of tanker trucks and rail), $\mathbb{P}^C$ is the carbon price, and λ^F is the GHG production rate from fuel use (GHG bookkeeping is described below). As mentioned above, $\tau_{rr'}$ for all other fuels is assumed to be the identity matrix. The total fuel *production* demand, $\mathbb{D}^{F^P}$, after accounting for ethanol exchange is,

$$\begin{aligned} \mathbb{D}^{F^P}_{rf} &= \sum_{r'} \tau_{rr'f} \mathbb{D}^F_{r'f} \\ \mathbb{D}^{F^P}_{r,diesel} &= \sum_{r'} \tau_{rr'f} \mathbb{D}^F_{r',diesel} + \sum_f \frac{\mathcal{X}_{rr'}}{\eta^F} \mathbb{D}^{F^P}_{rf}, \end{aligned}$$

where the diesel production demand is listed separately due to the additional demand stemming from the ethanol exchange.

The fuel production sub-model translates the regional fuel production demand to regional energy source demand via the relationship,

$$\mathbb{D}^E_{re} = \sum_f \Omega^F_{ref} \mathbb{D}^{F^P}_{rf},$$

where $\mathbb{D}^E$ is the energy source demand and Ω^F_{ref} is a matrix relating quantities of energy source, e, required to produce one unit of fuel, f. This matrix varies by state for electricity, due to the different grid mixes, and ethanol, due to the different breakdowns between grain and cellulosic ethanol production to satisfy RFS. For all other fuels, Ω^F does not vary by state. The entries into the matrix are taken from Wang [39].

As alluded to above, the fuel production sub-model also does an accounting of the GHG emissions due to fuel use and production, $\mathcal{G}$,

$$\mathcal{G}_{rf} = \lambda^F_f \mathbb{D}^{F^P}_{rf} + \lambda^C_{rf} \mathbb{D}^{F^P}_{rf}$$

where λ^F_f is the CO_2-equivalent emissions rate for fuel use and λ^C_{rf} is the emissions rate for fuel production processes. As above, λ^C_{rf} only varies by state for electricity and ethanol production. For vehicles using electricity, it was assumed that,

$$\begin{aligned} \lambda^F_{f=elec} &= 0 \quad ; \\ \lambda^C_{r,f=elec} &= \frac{\sum_e \lambda^E_{re} \mathcal{Y}^m_{re}}{\sum_e \mathcal{Y}^m_{re}} \quad , \end{aligned}$$

where λ^E is the emissions rate for electricity generation and $\mathcal{Y}^m$ is the marginal capacity of the grid. The values of λ^F, λ^C, and λ^E are taken from Wang [39] as well. Note that this is not a life-cycle GHG accounting as contributions from vehicle manufacturing and energy source production are not included. However, the values of $\lambda^C_{r,f=EtOH}$ are deducted by $\lambda^F_{f=EtOH}$ as it is assumed that the CO_2-equivalent content in the fuel is pulled from the atmosphere while the biomass was growing.

Lastly, the fuel production sub-model outputs the price of fuel in each region. This is calculated as,

$$\mathbb{P}^F_{rhf} = \sum_e \mathcal{E}_{hef}\mathbb{P}^E_{re}\Omega^F_{ref} + \mathbb{P}^C\left(\lambda^F_f + \lambda^C_{rf}\right) + \mathcal{T}_{rf},$$

where $\mathbb{P}^E$ is the energy source price, $\mathcal{E}$ is a multiplier that adjusts the source price based on different uses (e.g. the price of natural gas differs from well-head, to electric power, to industrial uses), $\mathbb{P}^C$ is a user-specified price on GHG emissions, and $\mathcal{T}$ is the total accumulation of taxes, fees, conversion and distribution costs, and profit margin. Fuel taxes and fees are taken from the American Petroleum Institute [1], and the retailer profit margin is taken from Energy Information Administration [10]. State-dependent distribution and conversion costs were deduced by comparing actual fuel prices against model estimates from the above equation with all other factors included.

2.3 Electricity grid evolution

The 2012 EPA e-grid database [29] provides a list of all of the electric power generators in the United States by state, age, and primary fuel type. This list initialized the base capacity in our model, where the primary fuel type was re-categorized as one of oil, coal, natural gas, biomass, or a generalized zero-carbon class (including nuclear, hydro-electric, wind, solar, or other renewable sources). All generators were assumed to have a lifespan, L, of 40 years in the baseline case before they were retired from the mix. Since the decisions associated with opening new nuclear or renewable power stations can be complex, and often politically charged, no retirement was assumed for that source type. This assumption could also be interpreted as retirement of old capacity coinciding with the addition of new capacity for nuclear and renewable power generation. This evolution can be expressed as,

$$\frac{\mathrm{d}\mathcal{Y}_{a=L,re}}{\mathrm{d}t} = \begin{cases} -\mathcal{Y}_{a=L,re}, & e \in [\text{Oil, Coal, NG}] \\ 0, & \text{else} \end{cases} \quad ,$$

where $\mathcal{Y}$ is the base capacity. The base electric load in each state, $\mathcal{Z}$, was initialized with annual survey data from the EIA [9], and assumed to increase each time step at the same rate of population growth. This base load, however, does not include the electricity demand for electric vehicle recharging, which was tracked separately,

$$\frac{\mathrm{d}\mathcal{Z}_r}{\mathrm{d}t} = (\mathcal{S} - \mathcal{W})\,\mathcal{Z}_r \quad .$$

As total demand, including vehicle recharging, increases beyond available capacity, new generators are added,

$$\frac{\mathrm{d}\mathcal{Y}_{a=0,re}}{\mathrm{d}t} = \psi_{re}\max\left[0, c\left(\mathbb{D}^{F^P}_{r,f=elec} + \mathcal{Z}_r - \sum_{ae}\mathcal{Y}_{are}\right)\right],$$

where ψ is the source type choice for new generators, and the scaling factor, c, ensures that the capacity added will exceed the deficit with some margin. The source type added to the capacity mix is assumed to be a decision based solely on price. Unlike the logit choice model mentioned frequently above, in this choice only one source type is selected per state. This assumption is meant to reflect the large capital expenditure required to build new capacity, such that the investment is only made in one source type at a time,

$$\psi_{re} = \arg\min_e \left[\left(\Omega^E_{ee}\mathbb{P}^E_{re} + \mathbf{A}\left(\mathcal{C}^{Cap}_e\right) + \mathcal{C}^{OM} + \epsilon_e\right] \quad \forall r \quad ,$$

where Ω^E is the conversion efficiency matrix for electricity production from a given primary feedstock, $\mathcal{C}^{Cap}$ is the capital cost of building new capacity per unit energy, $\mathcal{C}^{OM}$ is the operations and maintenance cost per unit energy, and ϵ is a random number to recognize that new capacity is not always selected according to the absolute lowest price per unit energy. Amortization of the capital cost is done over the generator lifespan, L, at discount rate of 7%. Cost data for new capacity was taken from Drennen and Andruski [7].

The base electric capacity mix in each state determined the price of electricity and the carbon intensity for industrial electricity usage, such as the use of electricity in the refining of gasoline. Electric vehicles, and their associated GHG emissions, were assumed to be supplied by the marginal capacity available in a given state. It was assumed that electric power from oil, coal, and natural gas could most easily scale to meet off-peak charging demand [17]. Thus, the biomass and zero-carbon fueled electricity supplied the base demand first.

2.4 Modeling energy sources

The US Department of Energy's Annual Energy Outlook reference case was our source for crude oil, coal, and natural gas prices [36]. Crude oil and coal were assumed to be global and national commodities, respectively, with prices unaffected by perturbations in US LDV fuel demand. Natural gas prices, as reported by the EIA, varied by region, but were similarly assumed to be unaffected by the LDV fleet. Renewable energy pricing was derived from the ReEDS model [26]. Biomass supply curves were constructed from the US Billion-Ton Update analysis [31]. The somewhat notional price points for the various feedstocks in the Billion-Ton data were corrected to more accurately reflect current markets. All of the feedstocks were then aggregated together to create a single biomass supply curve in each state. Finally, separate grain-based and cellulosic-based supply curves were also constructed so that the relative ratio of those two types could be ascertained for a given price point.

This page intentionally left blank.

Chapter 3

Numerical analysis

This chapter presents the parametric analysis results obtained using the model. Model parameterization and output metrics of interest are discussed. Results are shown for both a global sensitivity analysis and more focused trade space studies, using the metrics of GHG emissions and petroleum consumption.

It is worth noting that this analysis focuses on policies that could influence vehicle *buying* behavior, but not *driving* behavior. Population migration away from suburbs and into urban enclaves or mass-transit improvements could decrease VMT, GHG emissions, and petroleum consumption as well, but are not considered here.

3.1 Model parameterization

Overall, the model parameterization spans variables that could be categorized across multiple conceptual labels, such as inherent modeling assumptions, economic forecasting, technological development, and future policy decisions. It is not feasible to independently parameterize every single input variable in the model both due to variable inter-dependency and also tractability of the sensitivity analysis. Instead of varying the crude oil price in 2030 and 2031 independently, for instance, all oil prices are scaled by a multiplier that varies from 1 in 2010 to a user-specified value in 2050. This *multiplier* approach is similarly applied to other energy source supply curves, vehicle efficiency data, battery costs, and consumer choice penalties. Where appropriate, such as the exponent in the logit choice function, individual variables are parameterized directly. The key parameterization of the electricity grid, aside from the energy feedstock prices, is the generator lifespan.

Uniform distributions are assumed for all parameters in all studies. For the sensitivity analysis, parameter minimums, maximums, and baseline values are described in Table 3.1. The carbon price parameter appends an additional cost to fuels proportional to the emission of GHG and represents a potential carbon tax policy. For calibration, the maximum carbon price considered, \$1,000 per metric ton of CO_2 equivalent, corresponds to an additional price on gasoline of nearly \$10 per gallon. Two other parameters, the consumer payback period and the penalty multiplier, could also be considered variables subject to policy influence. The energy supply multipliers (for biomass, zero-carbon, coal, natural gas, and oil) address commodity forecasting uncertainty. A number of parameters included in the sensitivity analysis characterize the uncertainty in technological development. Technological performance uncertainty is captured by multipliers applied to ICE powertrain efficiency, electric powertrain efficiency, and home charger costs. Similarly, the variation in battery cost can be thought of as the technological maturation of battery storage and manufacturing. The uncertainty associated with infrastructure development is captured by the refueling station growth rate parameter. Finally, the remaining parameters included in the sensitivity analysis are notable model assumptions with the potential for influencing output metrics. These include the three logit choice exponents (for vehicle selection, fuel selection for FFVs, and ethanol exchange), the overall fleet growth rate, and the overall vehicle sales rate which, together with the fleet growth rate, also determines the overall scrap rate.

It should be noted that all of the input parameters are assumed to be independent. While this assumption is plausible near the baseline values, it is likely less valid at some value extremes. For instance, at high values

Table 3.1. Baseline values and uniform distribution ranges for sensitivity analysis parameters.

Parameter	Baseline	Min	Max
Carbon price [$/MT CO_2 equivalent]	0	0	1000
Consumer payback period [years]	3	2	11
Penalty multiplier	1	0	1
Battery cost multiplier	1	0.1	2
Charger cost reduction [per year]	3%	0%	6%
ICE powertrain eff multiplier	1	1	3
Electric powertrain eff multiplier	1	1	3
Electricity generator lifespan [years]	40	10	70
Vehicle choice logit exponent	[9,12,15]	[2.4,3.2,4]	[12,16,20]
Bi-fuel choice logit exponent	18	2	20
Ethanol transport logit exponent	18	2	20
Fleet growth rate	0.9%	0.5%	2.0%
Vehicle sales rate	6.7%	5%	9%
Refueling station growth [per 1k new vehicles]	0.7	0.01	2
Oil price multiplier	1	0.5	3
Coal price multiplier	1	0.5	3
Natural gas price multiplier	1	0.5	3
Biomass price multiplier	1	0.5	3
Renewable energy price multiplier	1	0.25	3

of oil price or carbon price, consumers would probably have longer payback periods than current estimates. Similarly, battery costs and electric powertrain efficiency are likely coupled, as high efficiency might be associated with higher battery costs.

3.2 Output metrics of interest

The first metric of interest is LDV fleet fractions of ICEs and EVs, where ICEs are all the internal-combustion powertrains that do not tap into the electricity grid, and EVs are defined as the sum of PHEVs and BEVs. In his 2011 State of the Union address, President Barack Obama promulgated a national goal to have one million EVs on the roads in the US by 2015 [21]. Since 1 million vehicles represent less than 1% of the total fleet, small changes in parameter values can have a significant impact on meeting this target.

To address the environmental perspective of transportation energy, we examine the relationship between the LDV fleet and GHG emissions. The model is capable of tracking GHG emissions, specifically the quantity of carbon dioxide equivalent emissions released into the atmosphere either through direct LDV fleet tailpipe emissions or indirectly through fuel and electricity production. A number of organizations, states, and countries have set out ambitious GHG reduction goals for 2050. The State of California and the European Commission, for instance, have both targeted an 80% reduction in CO_2 below 1990 emissions levels by 2050 [11, 25]. A recent study by Grimes-Casey et al. [16] distributed the IPCC-recommended global carbon reduction targets to individual countries and sectors based on population and economic modeling. They determined that the average US LDV well-to-wheel GHG emissions must be reduced 88% in 2050 over 2002 levels. Despite these mandates, CO_2 emissions have nevertheless increased from 1990 to 2010 [5]. To distance our GHG analysis from assumptions of fleet growth rate, we consider GHG reductions per mile traveled by the fleet using a 2010 reference point.

To address the security context of energy use, we examine the total petroleum consumption from the LDV transportation sector, and its corresponding relationship to imported crude oil. Reducing petroleum consumption significantly could enhance US energy security by mitigating dependency on foreign sources.

Similar to the GHG case, we examine petroleum demand per mile traveled by the fleet using a 2010 reference point.

3.3 Baseline model predictions

Before presenting the parametric analysis studies, it is helpful to understand the baseline model state about which variations are taken. As stated above and illustrated in Figure 3.1a, the average LDV fleet fuel economy is projected to improve markedly from 2010 to 2050, with a more than 50% decrease in total fuel consumption. Concurrently, battery costs are expected to decrease by more than 80%, shown in Figure 3.1b, due to technological maturation. Similar to the sensitivity analysis, these cost and efficiency values are scaled parametrically through the multiplier approach to explore their dynamics, critical points, and tradeoffs. The range of values surveyed by the multipliers are the shaded regions in Figures 3.1a–b.

The baseline model outputs are also shown in Figure 3.1. For the baseline model state, fleet breakdown by vehicle powertrain over time is drawn in Figure 3.1c. In this projection, pure ICE powertrains and conventional hybrid powertrains are a nearly 60% of the fleet; PHEV10s are more numerous than PHEV40s, and BEVs are less than 10% of the fleet. This pace of EV growth is slightly below the required pace to meet Obama's EV target in 2015, shown in Figure 3.1d. Interestingly, the impact of federal and state subsidies on EV sales is significant. With subsidies, the baseline model state predicts 2–3 times more EVs than would otherwise be on the road from 2015-2020.

As a fraction of 2010 quantities, reductions in GHG emissions per fleet mile are shown in Figure 3.1e. For this quantity, the model projects a baseline reduction of 50% by 2050. The petroleum consumption per fleet mile shows an even greater baseline reduction, in Figure 3.1f, of nearly 65% by 2050.

3.4 Sensitivity analysis

A sensitivity analysis was performed to verify expected model behavior and to reveal the most significant drivers of variability in output metrics of interest. To account for complex variable interactions, as well as large changes to non-normalized input and output variables, a non-parametric, non-linear global sensitivity analysis was performed. Specifically, a Monte Carlo simulation allowed the uncertain input parameters listed in Table 3.1 to vary. Spearman rank correlation coefficients were then computed between the output metrics of interest and the input parameters. The magnitude of the correlation coefficient relates the degree to which a given input parameter variance is statistically associated with an output variance. A coefficient value of 1 or -1 represents a perfect positive or negative correlation, respectively. A Monte Carlo simulation with 1,250 model evaluations and Latin hypercube sampling generated the sensitivity analysis sample data. A follow-on Monte Carlo simulation with 2,500 model evaluations confirmed convergence of the results. The sensitivity analysis results are described in Table 3.2 where each value represents the Spearman rank correlation coefficient of an output metric, listed in columns, with respect to an input parameter, listed by rows.

The sensitivity analysis for LDV GHG emissions per mile in 2050 shows that the parameters that drive the composition of the fleet and the GHG intensity of each mile traveled are the most influential. The parameters that determine the composition of the fleet include the consumer payback period, vehicle sales rate, and logit choice exponent. Similarly, the price of carbon-intensive fuels influences the composition of the fleet, hence the significance of the carbon price and oil price multiplier parameters. Finally, both the ICE and electric powertrain efficiency multipliers have a noteworthy impact. The electric generator lifespan, which has the highest correlation coefficient for per mile GHG emissions, can be viewed as the parameter that determines the GHG efficiency of the grid. The sooner coal and oil-based generators are retired and replaced with natural gas (due to its low price projections), the more EVs will have an impact on GHG emissions.

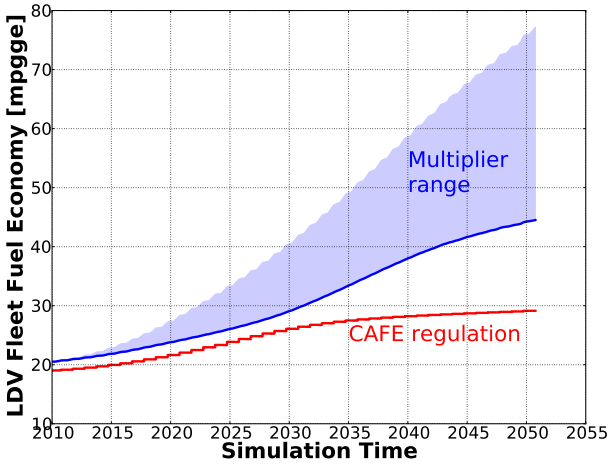

(a) Baseline fleet fuel economy

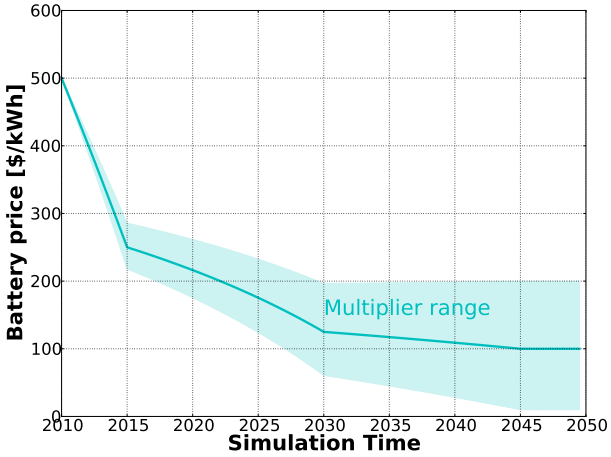

(b) Baseline battery costs

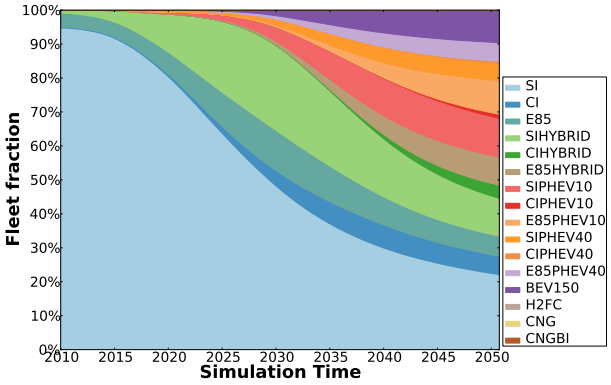

(c) Baseline fleet fractions

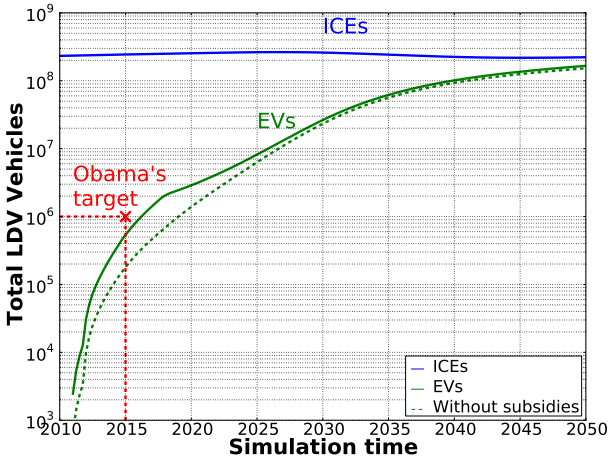

(d) Baseline EV market penetration

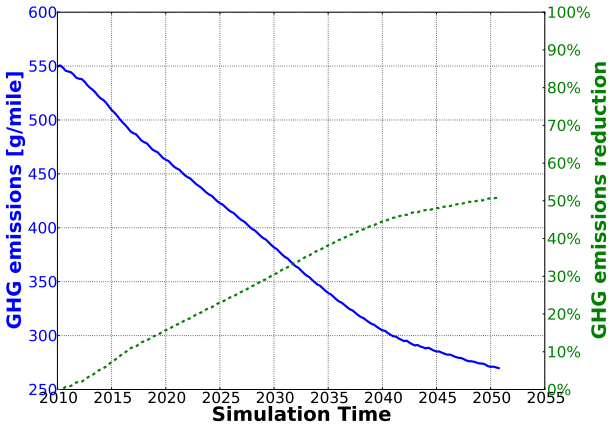

(e) Baseline GHG emissions

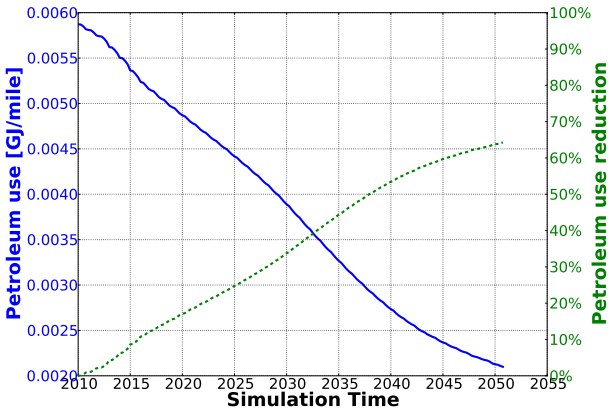

(f) Baseline petroleum consumption

Figure 3.1. Baseline efficiency, battery costs, fleet fractions, GHG emissions, and petroleum consumption.

Table 3.2. Spearman rank correlation coefficients for outputs (columns) with respect to inputs (rows). Output metrics are measured at simulation end, 2050.

Parameter	GHG/mile emissions	Petrol/mile consumption	ICE fleet fraction	BEV150 fleet fraction
Carbon price	-0.21	-0.26	-0.26	0.32
Consumer payback period	-0.31	-0.45	-0.48	0.49
Penalty mult	0.05	0.06	0.07	-0.17
Battery cost mult	0.13	0.20	0.22	-0.48
Charger cost reduction	0.01	0.02	-0.04	0.04
ICE powertrain eff mult	-0.20	-0.02	0.49	-0.47
Electric powertrain eff mult	-0.28	-0.11	-0.07	0.14
Electricity generator life	0.48	-0.02	0.08	-0.09
Max vehicle choice logit exp	-0.26	-0.36	-0.34	0.14
Bi-fuel choice logit exp	-0.03	-0.07	0.09	-0.07
Ethanol transport logit exp	0.00	0.03	0.04	-0.03
Fleet growth rate	0.00	0.00	-0.05	0.05
Vehicle sales rate	-0.36	-0.40	-0.41	0.17
Refueling station growth	-0.03	-0.04	0.01	-0.05
Oil price mult	-0.23	-0.39	-0.21	0.20
Coal price mult	-0.01	0.01	0.01	0.01
Natural gas price mult	-0.02	0.04	0.03	-0.06
Biomass price mult	0.03	0.05	0.02	-0.05
Zero-carbon price mult	0.02	-0.01	-0.01	0.0

Table 3.2 also lists the sensitivity analysis results for LDV petroleum consumption per fleet mile in 2050. The results are similar to those for LDV GHG emissions. In this case, however, the correlations for the parameters related to efficiency have decreased dramatically and those related to the composition of the fleet have increased. This is underscored by the nearly identical correlation coefficients for per mile petroleum consumption and final ICE fleet fractions in 2050. It is interesting to note that for both of these outputs, consumer payback period becomes one of the most influential parameters and battery cost begins to demonstrate significance as well.

Although the sensitivity analysis results for the total EV fleet fraction are identical to the ICE results (since the two categories are complementary), the BEV fleet fraction in 2050 is extracted and shown in Table 3.2. In this case, a few additional parameters, in addition to those correlated with ICE fleet fractions, show signs of notable influence. These include electric powertrain efficiency and consumer penalties. This larger suite of parameters perhaps reflects that a potential BEV customer must both choose not to purchase an ICE, and also to single out BEVs from the PHEVs. One conclusion that could be drawn from this sensitivity analysis is that there are many factors that contribute to the adoption of BEVs, and EVs in general. Technology improvements or policy initiatives in isolation cannot effect widespread change. Only through the combination of improvements in multiple technologies with broad policy incentives and direct subsidies will EVs play a significant role in the LDV fleet.

3.5 Trade space analysis

3.5.1 Electric vehicle adoption targets

More detailed parametric studies, beyond the sensitivity analysis, were conducted to understand the penetration of electric vehicles into the LDV fleet. Figure 3.2a depicts the impact of two market-based adjustments

that might be available to policy makers to influence the fleet fraction of EVs in 2050. The consumer payback period can be influenced by media campaigns, consumer education, and even direct subsidies. In fact, adjusting consumers' perceived payback period from 3 to 9 years can increase the EV fleet fraction by 20 percentage points. Carbon price, as a disincentive for fossil fuel consumption, can change the EV fleet fraction by approximately 15 percentage points for the range of values considered, a slightly less influential parameter in this respect than the payback period.

It is interesting to compare the competing influences of electric powertrain efficiency and the consumer payback period upon the adoption rates of EVs, which is displayed in Figure 3.2b. Surprisingly, the contour lines are almost chiefly aligned with the payback period axis. Even if electric powertrain efficiency is twice baseline projections, our model predicts that the impact on EV sales rates will be negligible. The difference in price between traditional vehicles and EVs stems from the batteries themselves, immature manufacturing processes, and perceived range and infrastructure penalties for BEVs. Improving electric powertrain efficiency only addresses the BEV range penalty component of the cost differential since we assumed that the total battery pack capacity remained constant. Furthermore, even if battery costs are decreased significantly, as shown in Figures 3.2c–d, there is no corresponding leap in the EV fleet fraction. Essentially, there will always be a price differential between traditional vehicles and EVs. Only if consumers consider the aggregated fuel costs savings over the lifetime of the vehicle (i.e. increasing the consumer payback period) will EVs become attractive based on cost. As suggested by Figure 3.2c, the break-even point between up-front capital costs and fuel cost savings is sensitive to the price of oil and other unknown costs, such as battery costs.

Figure 3.2d also shows the impact of ICE powertrain efficiency on EV fleet fraction. While increased ICE powertrain efficiency decreases the EV fleet fraction, since EVs become less attractive, the impact is small. Increasing ICE powertrain efficiency, perhaps contrary to common opinion, is not entirely antithetical to increased EV adoption as ICE powertrain efficiency gains benefit the PHEVs as well.

At extreme values of the parameter space, the fleet fraction of EVs can reach nearly 80%. While these tradeoff explorations can guide decision makers to encourage EV sales, one must also question if EV fleet penetration is a worthy goal in its own right. Perhaps environmental or security objectives should be targeted directly? To that end, our model can simulate a future with and without EVs by effectively turning them on or off. This comparison uncovers the benefit of EVs upon other metrics of interest. Figure 3.3 shows the reduction in GHG emissions and LDV petroleum consumption per mile for this tradeoff versus variations in ICE powertrain efficiency. The first observation from these plots is that the value of EVs is somewhat subject to the performance uncertainty of future ICE powertrains. If unanticipated technological leaps are made in ICE powertrain efficiency, then EVs will indeed have limited utility. If technology improvements are consistent with baseline projects, then EVs can offer noticeable savings for GHG emissions of up to 10% percentage points and petroleum consumption of nearly 20% percentage points. These conclusions are dependent on the assumption that the electricity grid is anticipated to become less carbon-intensive in this same time frame.

3.5.2 Reduction in greenhouse gas emissions per mile

The model baseline already projects a GHG per mile reduction of 50% below 2010 values by 2050, but the LDV segment must do more if the 80% reduction targets below 1990 levels are to be achieved. If policy makers relied upon market-based influences only, as shown in Figure 3.4a, then the reduction targets are feasible, albeit at carbon prices that some might consider extreme. Interestingly, the contours in Figure 3.4a suggest that consumer payback period has limited leverage over GHG emissions at low carbon prices, but at much higher carbon prices it becomes quite influential. This suggests that from the baseline starting point, the most effective market policy is to initiate a carbon tax. From a technology point of view, tradeoffs with both ICE and electric powertrain efficiencies are shown in Figure 3.4b–d. Of these two, ICE powertrain efficiency is clearly the bigger driver of GHG reductions. For electric powertrain efficiency to effect noteworthy GHG reductions, it must realize extreme values and be coupled with significant extensions in consumer payback period.

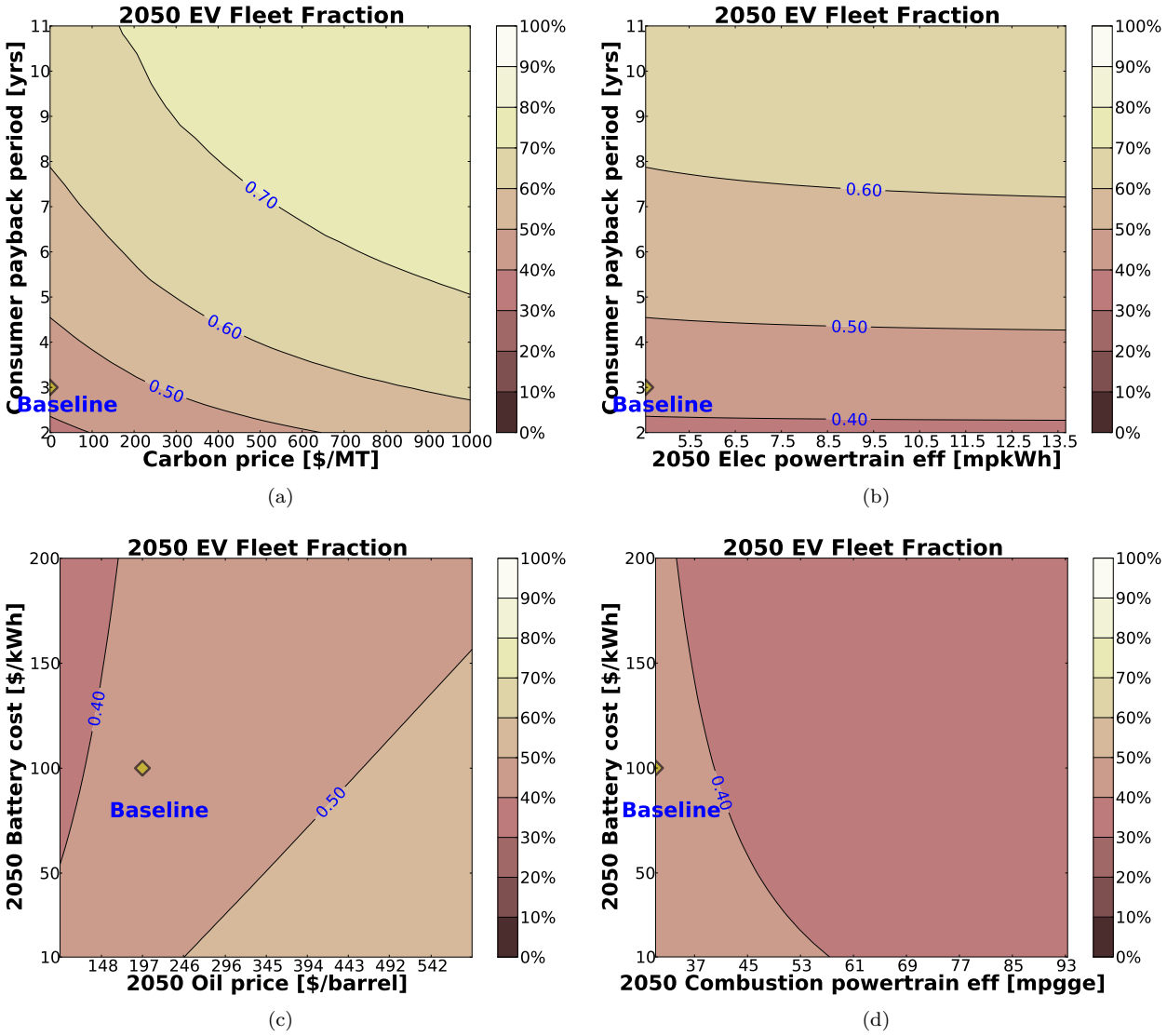

Figure 3.2. Contours of electric vehicle fleet fractions. Efficiencies listed are for compact cars. *Baseline* represents initial values in the model for the x and y variables.

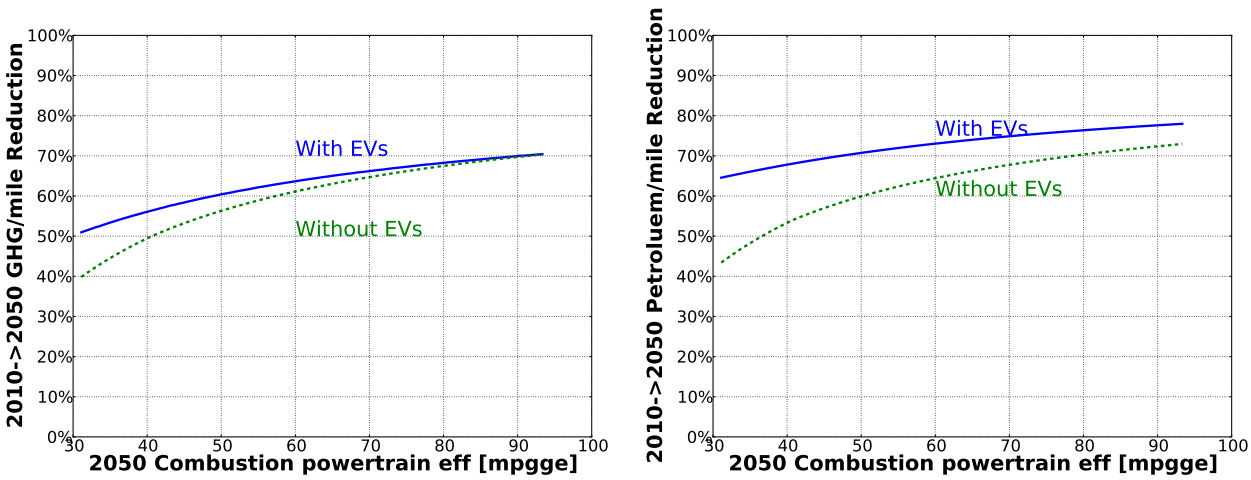

Figure 3.3. Overall contribution of electric vehicles to reductions in GHG and petroleum consumption per fleet mile in 2050, relative to 2010. Efficiencies listed are for compact cars.

The impacts of ICE powertrain efficiency and battery cost changes are shown in Figure 3.4b. As one would expect, the contour lines are nearly aligned with the ICE powertrain efficiency axis. This suggests that meeting the most ambitious GHG reduction targets requires, chiefly, improvement in ICE powertrain efficiencies and that battery costs have little impact on GHG emissions. Additionally, the 80% reduction target falls at ICE powertrain efficiencies beyond 95 mpg for compact SI cars, nearly triple the baseline projection. Thus, meeting the most aggressive targets might be dependent upon realizing technological leaps or currently unforeseen advances, rather than incremental changes.

The results in Figures 3.2a and 3.4a suggest that policies focused on direct carbon pricing and consumer payback periods could lead to a fleet comprised of more than 70% EVs, and that this fleet could meet the most aggressive GHG reduction targets. However, since there is skepticism that the US will adopt a carbon price directory, the parameter space that leads to increased EV adoption rates was explored in more depth. We consider a world that is ideal for the purchase of EVs: consumer payback periods are tripled, batteries are nearly free, consumer range and infrastructure penalties for BEVs are eliminated, and a high vehicle turnover rate ensures that the oldest, least efficient vehicles are replaced with higher efficiency models quickly. Furthermore, this ideal environment rapidly retires the coal intensive sources of electricity within the next 5 years in favor of natural gas. In this setting, depicted in Figure 3.5, ICEs still remain 20% of the fleet in 2050, and the EVs are dominated by PHEV10s and BEVs since PHEV40s are the most expensive powertrain. Additionally, of all of the vehicle-miles traveled, nearly 30% of them are still powered by liquid fuels due to the many PHEV10s. Therefore, the GHG per mile reduction in 2050 is only 65% over 2010 values, still short of the available improvement offered by the range of ICE powertrain efficiencies considered. Thus, to meet the most aggressive GHG reduction targets, ICE powertrain efficiency improvements beyond current projections are critical even for a fleet that consists of 80% EVs. Only by recharging the EVs with carbon free sources, such as wind or nuclear, can the 80% GHG reduction target per mile be achieved using default projections for ICE powertrain efficiency. In short, many unlikely parameter values must be realized for EVs to drive compliance with the most aggressive GHG reduction targets.

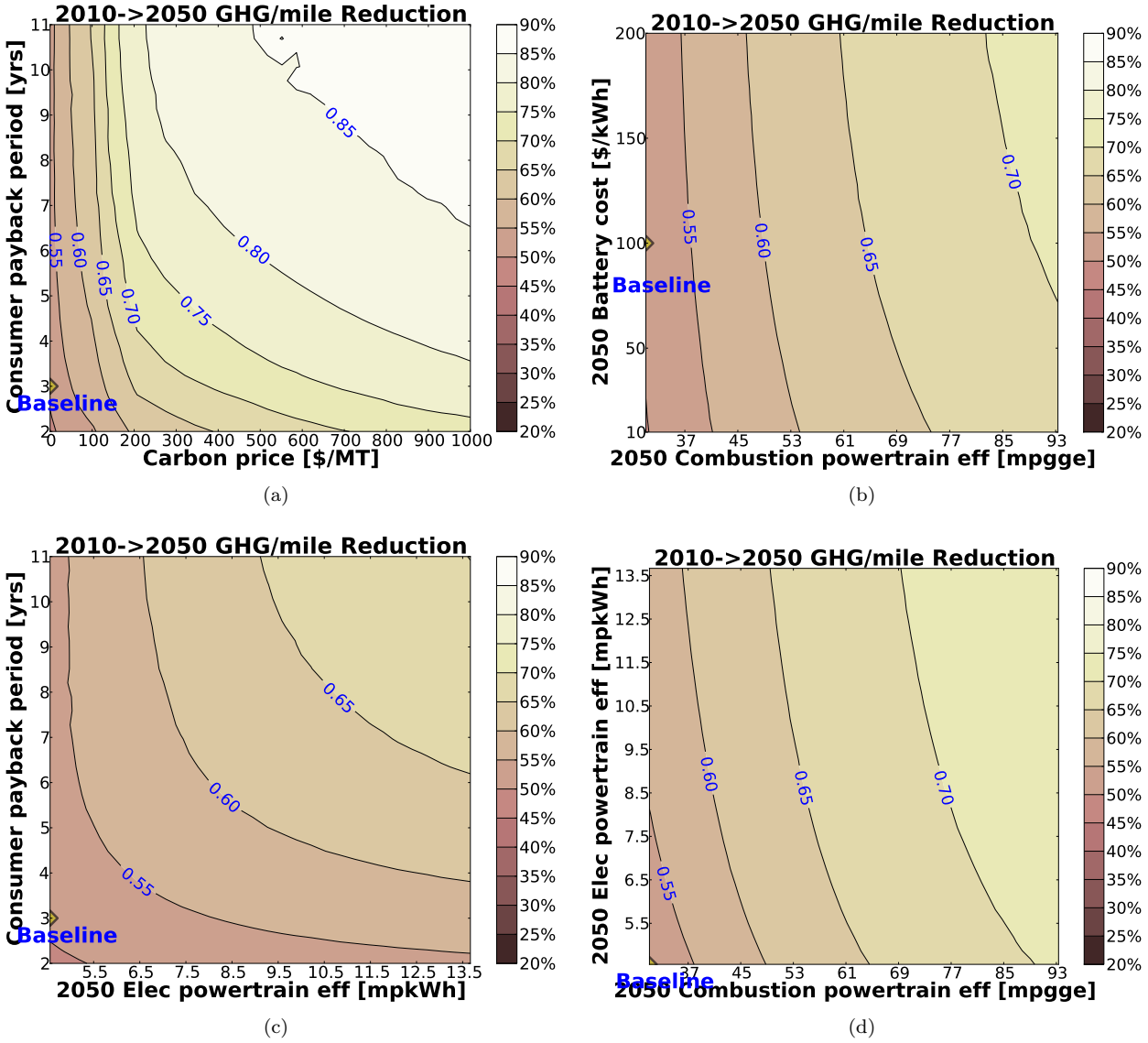

Figure 3.4. Contours of LDV GHG reduction per fleet mile in 2050 relative to 2010. Efficiencies listed are for compact cars. *Baseline* represents initial values in the model for the x and y variables.

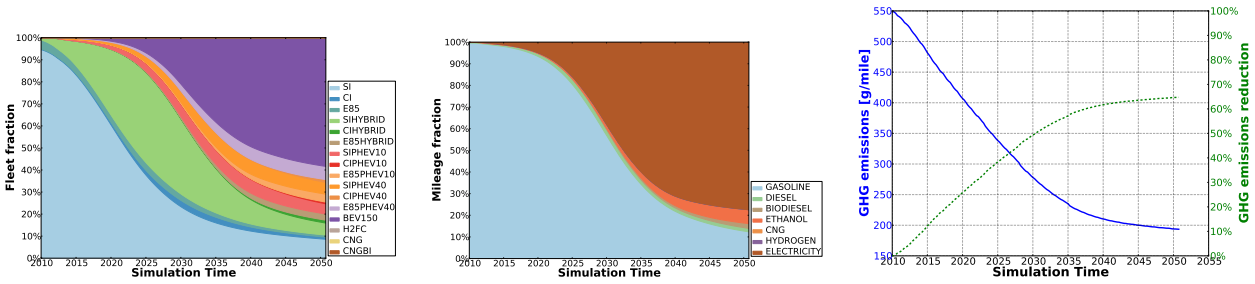

(a) (b) (c)

Figure 3.5. Fleet fractions, energy mileage fractions, and per mile GHG reductions under ideal conditions for electric vehicle adoption.

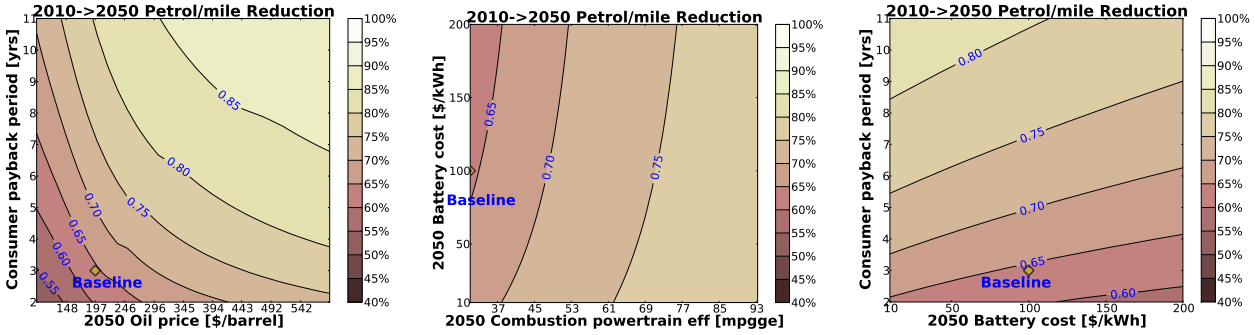

(a) (b) (c)

Figure 3.6. Contours of LDV petroleum consumption reduction per mile in 2050 relative to 2010. Efficiencies listed are for compact cars. *Baseline* represents initial values in the model for the x and y variables.

3.5.3 Reduction in petroleum consumption

The model baseline projects a more than 60% reduction in petroleum consumption per mile in 2050 over 2010 levels, due to improved vehicle efficiencies and electrification of the fleet. The parametric variations that further increase either vehicle efficiency or EV sales will therefore result in even lower petroleum consumption. For instance, market-based influences such as consumer payback period and market uncertainties, such as high oil prices, both serve to encourage vehicle electrification and reduce petroleum consumption. As depicted in Figure 3.6a, at the extreme values of consumer payback period and oil price, petroleum consumption reduction per mile can reach nearly 90%.

Technological influences upon LDV petroleum consumption are shown in Figure 3.6b. As one would expect, ICE powertrain efficiency improvements offer significant opportunity for reducing petroleum consumption, but unlike the GHG reduction case, the contour lines are not wholly aligned with the ICE powertrain efficiency-axis. In this case, lower battery costs also augment EV sales rates, especially at lower values of ICE powertrain efficiency, and therefore reduce average vehicle petroleum consumption. Thus, the US can meet aggressive petroleum consumption reduction targets without relying chiefly on improvements to ICE powertrain efficiency. This is underscored in Figure 3.6c where consumer payback period incentives are combined with battery technology improvements. At low battery costs and long consumer payback periods,

2050 average vehicle petroleum consumption is reduced by more than 80% over 2010 values.

This page intentionally left blank.

Chapter 4

Conclusions

The parametric analysis capability of the model presented here is new to this application space. This capability has enabled a comprehensive sensitivity analysis and trade space exploration, with emphasis on factors that influence the adoption rates of EVs, the reduction of GHG emissions, and the reduction of petroleum consumption within the US LDV fleet.

Many factors contribute to the adoption rates of EVs. These include the pace of technological development for the electric powertrain, battery performance, as well as ICE powertrain efficiency. Policy initiatives can also have a dramatic impact on the degree of EV adoption. The consumer payback period, in particular, can increase the EV fleet fraction if extended towards the lifetime of the vehicle. Widespread EV adoption can have noticeable impact on GHG emissions, assuming the electricity grid shifts away from coal, but the level of reduction is still short of stated targets. Similarly, widespread EV adoption can also reduce petroleum consumption by the LDV fleet and assist in reducing US reliance on imported crude oil.

The conventional, liquid-fueled internal combustion vehicle will remain the core of the LDV fleet for many years to come. This conclusion seems robust even if global oil prices rise to two to three times current projections. Thus, investment in improving the internal combustion engine might be the cheapest, lowest risk avenue towards meeting ambitious GHG emission and petroleum consumption reduction targets out to 2050. Vehicle efficiency improvements, however, will have to be negotiated with historical consumer and manufacturer preferences for large, powerful cars with many energy-hungry cabin features.

This page intentionally left blank.

Chapter 5

Analysis of fuel consumption trends in construction projects

To expand upon the light-duty vehicle analysis, we conducted preliminary analysis of fuel consumption trends by heavy-duty vehicles. Because of the breadth of heavy-duty vehicles and their diverse modes of use, we first focused on fuel consumption for heavy-duty vehicles and equipment used in construction projects. Recent estimates of fuel consumption in construction projects are highly variable. Lack of standards for reporting at both the equipment and project levels make it difficult to quantify the magnitude of fuel consumption and the associated opportunities for efficiency improvements in construction projects. In this study, we examined clusters of Environmental Impact Reports for seemingly similar construction projects in California. We observed that construction projects are not characterized consistently by task or equipment. We found wide variations in estimates for fuel use in terms of tasks, equipment, and overall projects, which may be attributed in part to inconsistencies in methodology and parameter ranges. Our analysis suggests that standardizing fuel consumption reporting and estimation methodologies for construction projects would enable quantification of opportunities for efficiency improvements at both the equipment and project levels. With increasing emphasis on reducing fossil fuel consumption, it will be important to quantify opportunities to increase fuel efficiency, including across the construction sector. Details of the analysis can be found in Peters and Manley [23].

This page intentionally left blank.

References

[1] American Petroleum Institute. *Motor Fuel Taxes*, June 2012. URL `http://www.api.org/Oil-and-Natural-Gas-Overview/Industry-Economics/Fuel-Taxes.aspx`.

[2] Bandivadekar, Anup, Bodek, Kristian, Cheah, Lynette, Evans, Christopher, Groode, Tiffany, Heywood, John, Kassaeris, Emmanuel, Kromer, Matthew, and Weiss, Malcolm. "On the Road in 2035: Reducing Transportation's Petroleum Consumption and GHG Emissions." Report LFEE 2008-05 RP, Massachusetts Institute of Technology, July 2008.

[3] Barter, Garrett E., Reichmuth, David, Westbrook, Jessica, Malczynski, Leonard A., West, Todd H., Manley, Dawn K., Guzman, Katherine D., and Edwards, Donna M. "Parametric analysis of technology and policy tradeoffs for conventional and electric light-duty vehicles." *Energy Policy*, 46(0):473 – 488, 2012.

[4] Bureau, U.S. Census. "2010 Census of Population and Housing." Report, 2010.

[5] Butler, James H. *The NOAA Annual Greenhouse Gas Index (AGGI)*. National Oceanic & Atmospheric Administration, Boulder, CO, 2011. http://www.esrl.noaa.gov/gmd/aggi.

[6] Davis, Stacy C., Diegel, Susan W., and Boundy, Robert G. "Transportation Energy Data Book: Edition 30." Report ORNL-6986, Oak Ridge National Laboratory, June 2011.

[7] Drennen, Thomas E. and Andruski, Joel. "Power Systems Life Cycle Analysis Tool (Power LCAT)." Report SAND2012-0677, Sandia National Laboratories, May 2012.

[8] Elgowainy, A., Burnham, A., Wang, M., Molburg, J., and Rousseau, A. *Well-to-Wheels Energy Use and Greenhouse Gas Emissions Analysis of Plug-in Hybrid Electric Vehicles*. Argonne National Laboratory, Argonne, IL, 2009.

[9] Energy Information Administration. *Electric Power Annual 2010*. Washington, DC, November 2011.

[10] Energy Information Administration. *Gasoline and Diesel Fuel Update*, May 2012. URL `http://www.eia.gov/petroleum/gasdiesel/`.

[11] European Commission. "A Roadmap for moving to a competitive low carbon economy in 2050." August 2011.

[12] Greene, David L. "TAFV Alternative Fuels and Vehicle Choice Model Documentation." Report TM-2001/134, Oak Ridge National Laboratory, Oak Ridge, TN, 2001.

[13] Greene, David L., Baker, Howard H., and Plotkin, Steven E. *Reducing Greenhouse Gas Emissions from U.S. Transportation*. Pew Center for Global Climate Change, January 2011.

[14] Greene, David L. and Lin, Zhenhong. "Who Will More Likely Buy PHEV; A Detailed Market Segmentation Analysis." The 25th World Battery, Hybrid and Fuel Cell Electric Vehicle Symposium & Exhibition, November 2010.

[15] Greene, David L., Patterson, Philip D., Singh, Margaret, and Li, Jia. "Feebates, rebates and gas-guzzler taxes: a study of incentives for increased fuel economy." *Energy Policy*, 33(6):757–775, 2005.

[16] Grimes-Casey, Hilary G., Keoleian, Gregory A., and Willcox, Blair. "Carbon Emission Targets for Driving Sustainable Mobility with US Light-Duty Vehicles." *Environ. Sci. Technol.*, 43:585–590, 2009.

[17] Kromer, Matthew and Heywood, John. "Electric Powertrains: Opportunities and Challenges in the U.S. Light-Duty Vehicle Fleet." Report LFEE 2007-03, Massachusetts Institute of Technology, May 2007.

[18] Lin, Zhenhong and Greene, David L. "A Plug-In Hybrid Consumer Choice Model with Detailed Market Segmentation." Transportation Research Board 10-1698, 2010.

[19] Moawad, A., Sharer, P., and Rousseau, A. *Light-Duty Vehicle Fuel Consumption Displacement Potential up to 2045*. Argonne National Laboratory, Argonne, IL, July 2011.

[20] National Research Council. *Transitions to Alternative Transportation Technologies- Plug-In Hybrid Electric Vehicles*. National Academies Press, Washington, DC, 2010.

[21] Obama, Barack. "Remarks by the President in State of Union Address." The White House Office of the Press Secretary, January 2011.

[22] One Hundred and Tenth Congress of the United States of America. "Energy Independence and Security Act of 2007." Report H.R. 6, December 2007.

[23] Peters, Valerie A. and Manley, Dawn K. "An examination of fuel consumption trends in construction projects." *Energy Policy*, 2012. doi: 10.1016/j.enpol.2012.07.048.

[24] Plotkin, Steve and Singh, Margaret. *Multi-Path Transportation Futures Study: Vehicle Characterization and Scenario Analyses*. Argonne National Laboratory, Argonne, IL, July 2009.

[25] Schwarzenegger, Arnold. "Executive Order S-3-05." June 2005. The California Governor's Office.

[26] Short, Walter, Sullivan, Patrick, Mai, Trieu, Mowers, Matthew, Uriarte, Caroline, Blair, Nate, Heimiller, Donna, and Martinez, Andrew. "Regional Energy Deployment System (ReEDS)." Report NREL/TP-6A20-46534, Golden, CO, November 2011.

[27] Sissine, Fred. "Energy Independence and Security Act of 2007: A Summary of Major Provisions." Report, Congressional Research Service, 2007.

[28] Struben, Jeroen and Sterman, John D. "Transition challenges for alternative fuel vehicle and transportation systems." *Environment and Planning B: Planning and Design*, 35:1070–1097, 2008.

[29] TranSystems. "The Emissions & Generation Resource Integrated Database for 2012 (eGRID2012): Technical Support Document." Report, U.S. Environmental Protection Agency, Washington, DC, April 2012.

[30] U.S. Department of Energy. *Federal and State Laws and Incentives*, February 2011. URL `http://www.afdc.energy.gov/fuels/stations_counts.html`.

[31] U.S. Department of Energy. *U.S. Billion-Ton Update: Biomass Supply for a Bioenergy and Bioproducts Industry*. Number ORNL/TM-2011/224. R. D. Perlack and B. J. Stokes (Leads) Oak Ridge National Laboratory, Oak RIdge, TN, 2011.

[32] U.S. Department of Energy. *Alternative Fueling Station Counts by State*, August 2012. URL `http://www.afdc.energy.gov/laws/`.

[33] U.S. Department of Transportation Federal Highway Administration. "Highway Statistics 2009, State Motor-Vehicle Registrations." Report MV-1, MV-9, 2010.

[34] U.S. Department of Transportation Federal Highway Administration. *2009 National Household Travel Survey*, February 2011. URL `http://nhts.ornl.gov`.

[35] U.S. Department of Transportation National Highway Traffic Safety Administration. "Vehicle Survivability and Travel Mileage Schedules." Report DOT HS 809 952, Washington, DC, January 2006.

[36] U.S. Energy Information Administration. *Annual Energy Outlook 2012: with Projections to 2035*. U.S. Department of Energy, April 2012.

[37] U.S. Environmental Protection Agency. "Light-Duty Automotive Technology, Carbon Dioxide Emissions, and Fuel Economy Trends: 1975 Through 2009." Report 420-R-09-014, Washington, DC, 2009.

[38] U.S. Environmental Protection Agency and U.S. Department of Transportation. "2017-2025 Model Year Light-Duty Vehicle GHG Emissions and CAFE Standards: Supplemental Notice of Intent." Report 40 CFR Parts 85, 86, and 600, 2011.

[39] Wang, M. *GREET v1.8d*. Argonne National Laboratory, Argonne, IL, 2010. http://greet.es.anl.gov.

[40] Yacobucci, Brent D. and Capehart, Tom. "Selected Issues Related to an Expansion of the Renewable Fuel Standard (RFS)." Report, Congressional Research Service, 2008.

[41] Yeh, Sonia. "An empirical analysis on the adoption of alternative fuel vehicles: The case of natural gas vehicles." *Energy Policy*, 35(11):5865–5875, 2007.

DISTRIBUTION:

1	MS 0899	Technical Library, 8944 (electronic copy)
1	MS 0359	D. Chavez, LDRD Office, 1911

Sandia National Laboratories